Design of membrane actuator based on ferromagnetic shape memory alloy composite for synthetic jet applications

Yuanchang Liang [a,*], Yasuo Kuga [b], Minoru Taya [a]

[a] Center for Intelligent Materials and Systems, Department of Mechanical Engineering, University of Washington,
ME Building, Box 352600, Seattle 98105, WA, USA
[b] Department of Electrical Engineering, University of Washington, Seattle, WA, USA

Abstract

The active flow control (AFC) technology has been studied and shown that it can help aircraft improve aerodynamic performance and jet noise reduction. AFC can be achieved by a synthetic jet actuator injecting high momentum air into the airflow at the appropriate locations on aircraft wings. To produce strong synthetic jet flow at high frequency, a new membrane actuator based on ferromagnetic shape memory alloy (FSMA) composite and hybrid mechanism was designed and constructed. The hybrid mechanism is the stress-induced martensitic phase transformation caused by large force due to large magnetic field gradient, thus enhancing the displacement, as the stiffness of shape memory alloy reduces due to the martensitic transformation. This sequential event can take place within milliseconds. The high momentum airflow will be produced by the oscillation of the circular FSMA composite diaphragm close to its resonance frequency driven by electromagnets. Due to large force and martensitic transformation on the FSMA composite diaphragm, the membrane actuator that we designed can produce 190 m/s synthetic jets at 220 Hz.
© 2005 Published by Elsevier B.V.

Keywords: Synthetic jet actuator; Hybrid mechanism; Composite; Shape memory alloy; Ferromagnetic; Active flow control

1. Introduction

Many researchers have shown that active flow control (AFC) technology can help aircraft improve aerodynamic performance and jet noise reduction [1–8]. AFC can be achieved by the synthetic jet actuator injecting high momentum air into the airflow at the appropriate location (near the point of airflow separation) on aircraft wings. It will reattach the flow, increase lift and reduce the drag. Instead of steady blowing, the oscillated synthetic jet is more efficient and reliable to delay the flow separation [1–6]. This technology has been investigated and applied on the wings of rotorcrafts, for example, V-22 and VR-7, to increase their mission capability on both payload and range [9,11]. The performance of the synthetic jet can be determined by the dimensionless jet frequency (F^+) and the jet momentum coefficient C_u [11],

$$F^+ = \frac{f x_f}{U_\infty} \tag{1}$$

$$C_u = 2 \left(\frac{H}{c} \right) \left(\frac{U_j}{U_\infty} \right) \tag{2}$$

where f is the jet frequency, x_f the distance between the slot and the flap trailing edge [4], H the jet slot height, c the wing chord length, U_j the amplitude of the jet velocity and U_∞ is the free stream velocity. F^+ is generally from 1 to 10 and C_u is from 0.01 to 1% [1]. A conventional design of synthetic jet actuator is based on voice coil linear motor [10]. Most of the synthetic jet actuators have been constructed based on piezoelectric materials as actuator materials to produce synthetic jet flow [11–18]. Although these synthetic jet actuators can produce up to 100 m/s with frequency range of 300 Hz or higher, this may not strong enough for higher Mach number flight. Therefore, we are seeking another design approach of a synthetic jet actuator, which can produce much stronger synthetic jet flow with high frequency.

* Corresponding author. Tel.: +1 2066856722; fax: +1 2066164088.
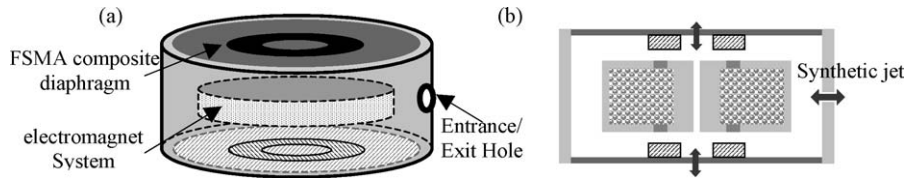 *E-mail address:* yliang@u.washington.edu (Y. Liang).

Fig. 1. (a) The schematic of the membrane actuator system for synthetic jet actuator, (b) the synthetic jet flow created by the oscillation of FSMA composite diaphragms.

Ferromagnetic shape memory alloys (FSMAs, i.e., Fe–Pd, NiMnGa) have been studied for possible applications of fast responsive and high power, yet light weight actuators controlled by magnetic field [19–21]. There are three approaches that have been proposed in the FSMA research community, (1) martensite variant mechanism by applied (constant) magnetic field (variant rearrangement mechanism used by the others) (2) magnetic (*H*) field induced phase transformation and (3) hybrid mechanism by applied magnetic field gradient. It is disadvantageous to use the first and the second approaches (constant magnetic field alone) to drive FSMAs because it has been found to produce small force [22–25]. We identified the third approach, hybrid mechanism [25], can produce large force and reasonably large stroke with fast response because it can be driven by a compact electromagnet with high-applied magnetic field gradient, providing a large stress capability, and reasonably large strain. Therefore, it is adopted in the present study of membrane actuators for the application to the synthetic jet actuator. The hybrid mechanism is based on the stress-induced martensitic phase transformation produced by applied magnetic field gradient, thus enhancing the displacement, as the stiffness of shape memory alloy reduces due to the martensitic phase transformation. Despite the promising performance of Fe–Pd FSMA system by the hybrid mechanism, the price of Pd is very expensive, thus, we have been searching for alternative FSMA materials. One of the alternative FSMA systems is a ferromagnetic shape memory alloy composite that consists of ferromagnetic material (such as soft iron) and superelastic grade shape memory alloy (such as NiTi). The function of the former is to introduce a large magnetic force by the hybrid mechanism, while that of the latter is to sustain large stress and induce larger strain. We have designed and fabricated the membrane actuator for the synthetic jet applications based on hybrid mechanism. It consists of an electromagnet system and a FSMA composite diaphragm made of superelastic grade of NiTi SMA thin sheet and ferromagnetic soft iron. This paper will present the design of the membrane actuator as well as its experimental results.

2. Concept and design of membrane actuator system

The membrane actuator mainly consists of a ferromagnetic shape memory alloy (FSMA) composite and an electromagnet system as shown in Fig. 1(a). The FSMA composite diaphragm is composed of a superelastic NiTi thin sheet and a ferromagnetic soft iron pad. The electromagnet system includes soft iron yoke laminate, magnet wire coil and permanent magnet, which can drive two composite diaphragms on both sides. As shown in Fig. 1(b), the composite diaphragm will be driven by the electromagnet system and oscillate to create synthetic jet flow through the entrance/exit hole. If the FSMA composite diaphragm oscillates close to its resonance frequency, its stroke can reach the maximum magnitude and produce strong synthetic jet flow, while the superelastic NiTi sheet can sustain large stresses without a permanent deformation. To achieve this operation, the resonance frequency of the composite diaphragm has to match closely with the magnetic field frequency response of the electromagnet system. Both the mechanical and electromagnetic finite element analyses are used for designing the optimum composite structure.

The dynamic analysis of the FSMA composite diaphragm is based on the finite element analysis, i.e., commercial code, ANSYS. Fig. 2(a) and (b) shows its ANSYS model and the side views of the composite diaphragm. The soft iron pad (30 mm × 32 mm × 3 mm) on each side of the composite diaphragm is square in order to obtain force from the electromagnet as large as possible. Two spacers are used between the soft iron pad and the NiTi sheet (64 mm in diameter and 0.3 mm in thickness) as shown in Fig. 2(b). Spacer#1 is a solid circular steel plate (33 mm in diameter and 1 mm in thickness) to maintain as a rigid body and to ensure the uniform stress distribution along the circumference on the NiTi sheet. This spacer also can be used to adjust the resonance frequency of the composite diaphragm depending on its dimension. Spacer#2 is made of aluminum (32 mm in diameter and 2 mm in thickness) and it is to prevent the contact between the soft iron pad and
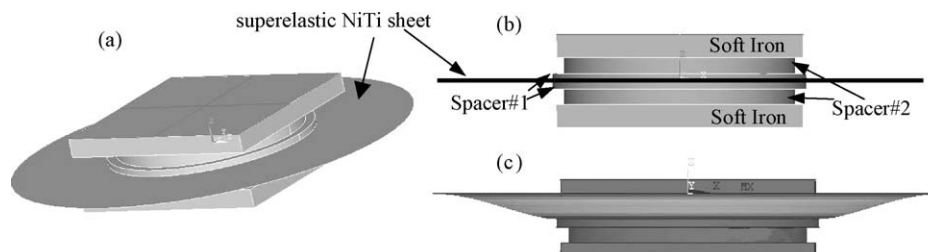

Fig. 2. (a) The FEM model of the FSMA composite diaphragm, (b) its size view, and (c) its deformation of static analysis.
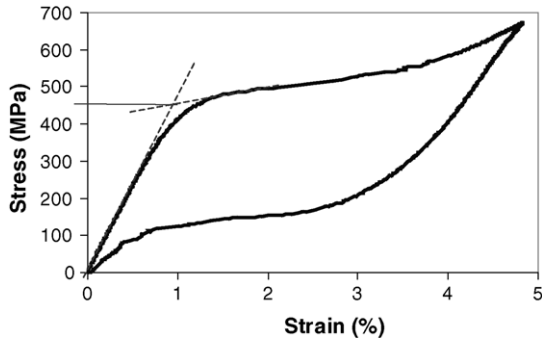
Fig. 3. The stress–strain curve of the 0.3 mm thick NiTi superelastic sheet.

Table 1
List of the material input data of the composite diaphragm for the FEM simulation

Material	Young's modulus (GPa)	Poisson ratio	Density (kg/m^3)
NiTi	55	0.33	6500
Soft iron	210	0.33	7850
Aluminum	70	0.33	2700

the NiTi sheet during the oscillation. In the FEM simulation, the boundary condition of the NiTi circular sheet is assumed to be totally constrained without rotation and slipping on its own diameter circumference and interface with the Spacer#1 circumference. The static analysis result is shown in Fig. 2(c). Since Spacer#1 is served as a rigid body, the deforming shape of the composite diaphragm is like a cone shape. The stress–strain curve of the superelastic NiTi sheet (0.3 mm thick) is used as the material input data as shown in Fig. 3. Because of the limitation of ANSYS FEA program, which can only perform the frequency response calculation with a linear Young's modulus, the estimation is only valid before the stress-induced martensitic transformation (at 450 MPa). However, this analysis result gives us a designing guidance of the composite diaphragm frequency we can drive. Table 1 lists the material input data for the FEM simulation.

Fig. 4 shows the examples of the FEA results. The dimensions of each layer of the composite diaphragm are described in the previous paragraph. We can vary the NiTi sheet thickness and obtain the resonance frequency of the composite diaphragm as a function of the NiTi sheet thickness is shown in Fig. 4(a), i.e., the
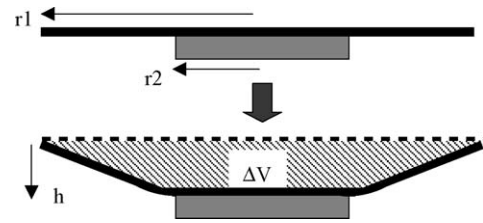
Fig. 5. Schematic of the deformation of the composite diaphragm.

thicker the sheet, the higher the resonance frequency becomes. The thickness of the soft iron pad also can change the resonance frequency of the entire composite diaphragm as well as the force level induced by the electromagnet because the larger volume of pad, the stronger force. Fig. 4(b) shows the results based on use of the thicker soft iron pad, results in lowering the resonance frequency of the composite diaphragm although a larger force can be obtained. Therefore, the optimization of the soft iron pad thickness is very critical. The simulation results also suggest that the highest stress level occurs on both locations of boundary condition as described above, i.e., the diameter circumference and the interface between the NiTi sheet and the pad. We have to assure that the stress level is near the onset of stress-induced martensitic transformation. Since the target frequency of the membrane actuator is between 150 and 250 Hz, the NiTi sheet thickness of 0.3 mm and the soft iron pad thickness of 3 mm are used. Please note that different combinations of the NiTi sheet thickness and diameter with a suitable size of soft iron pad can result in the same resonance frequency of the first mode on the composite diaphragm. We can estimate the jet flow velocity based on the deforming shape of the composite diaphragm (Fig. 2(c)), which is a cone shape. As shown in Fig. 5, $r1$ and $r2$ are the radius of NiTi plate and soft iron pad, respectively, and h is the stroke of the diaphragm. The volume change due to the deforming composite diaphragm can be calculated and synthetic jet flow velocity (v) can be estimated by the mass rate conservation:

$$v = \frac{\Delta V f}{WL} \quad (3)$$

where ΔV is the volume change, f the vibrating frequency of the composite diaphragm, W the width and L is the length of flow entrance/exit slot. For the current membrane actuator design
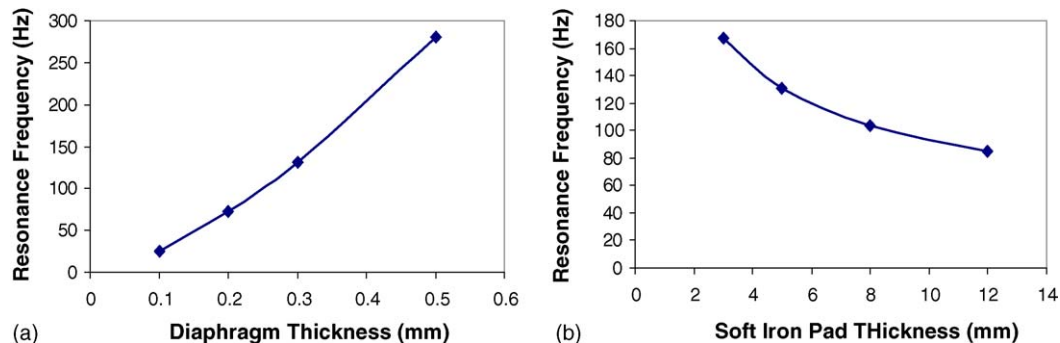

Fig. 4. (a) The thickness of the NiTi sheet (64 mm in diameter) and (b) the soft iron pad thickness (30 mm × 32 mm square area) estimated by FEM as a function of resonance frequency.
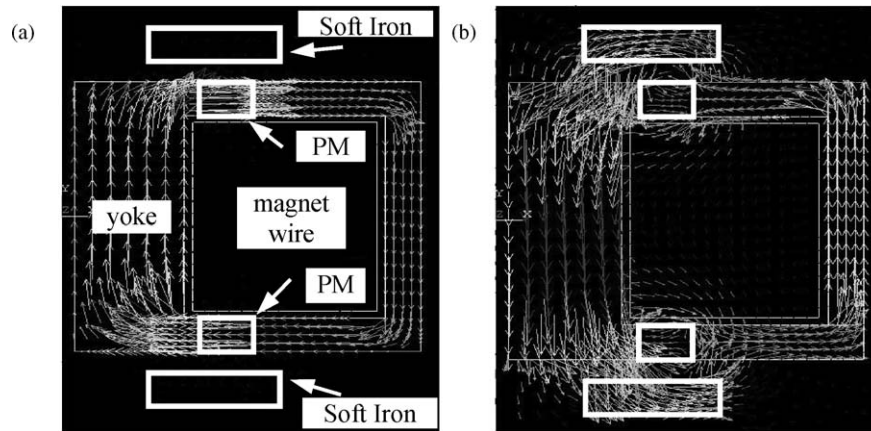
Fig. 6. Electromagnetic FEA results: (a) magnetic flux flows inside the yoke and no force is available on the soft iron when the power is off, (b) magnetic flux go through the soft iron pad and force is induced when the power is on.

($r1 = 32$ mm, $r2 = 16.5$ mm), if $h = 2$ mm, $f = 180$ Hz and the slot with $W = 1$ mm and $L = 5$ mm, the jet velocity is estimated about 275 m/s.

The FSMA composite diaphragm will be driven by a magnet system based on the concept of the hybrid magnet [26]. The system basically consists of permanent magnets, yoke and coils. It has been shown that the hybrid magnet system is more efficient and produces much larger force than the traditional solenoid magnet [27]. For the present case of the membrane actuator, we can modify the electromagnet system from one-side operation to both side operations, so two composite diaphragms can be driven by one system as shown in Fig. 6. This is an advantage if a series connection of several membrane actuators is needed for distributing the synthetic jet flow along the wing span. Fig. 6 shows the example of a 2D electromagnetic FEA model of the cylindrical electromagnet system. The model shows only the right half portion of the system due to its axisymmetric geometry. Both permanent magnets are polarized along their radius direction and made of Neodium (with Hc of 840 kA/m). It is noted that the polarized direction of the upper permanent magnet should be opposite to that of the bottom one, in order to establish an appropriated magnetic flux circuit. As shown in Fig. 6(a), when the power is off, most of magnetic flux (clockwise) produced by both permanent magnets flows inside the yoke. Therefore, no force is available on soft iron pads. When the power is on, Fig. 6(b), an opposite direction (counter clockwise) of magnetic flux is produced by input current. This new magnetic flux will force magnetic flux flowing out of the yoke around permanent magnets and produce a strong magnetic flux gradient. Then, the flux will go through soft iron pads and induce large force on both pads towards the electromagnet system. To ensure the high frequency use (200–300 Hz) and to increase the efficiency of the electromagnet system, the laminated yoke made of grain-oriented Fe–Si sheets is used. This is to eliminate the energy loss due to the eddy current effect and produce high magnetic field gradient resulting in strong force.

3. Testing results

Fig. 7(a) and (b) show the photo and parts of the membrane actuator, respectively. The overall size of the actuator is 72 mm × 85.6 mm × 130 mm and the total weight is 1.36 kg. It has two chambers in the center divided by the diaphragm. Each chamber has a 5 mm × 1 mm hole as the exit for the synthetic jet flow. The superelastic NiTi sheet of the composite diaphragm is cut by the EDM machine into a 72 mm in diameter circular sheet. Three different thicknesses, 0.2, 0.3 and 0.4 mm, are used. It will be clamped by two aluminum rings with 4 mm in width on both sides. Therefore, the effective diameter of the composite diaphragm is 64mm. Soft iron pads and Spacer#1 are made of 1018 low carbon steel with the size of 30 mm × 32 mm × 3 mm and 33 mm in diameter with 1 mm in thickness, respectively. Spacer#2 has the dimension of 32 mm in diameter and 2 mm in thickness. The finite element analysis shows that the resonance frequencies of the composite diaphragms of 0.2, 0.3 and 0.4 mm thickness are about 180, 200 and 220 Hz, respectively. Currently,
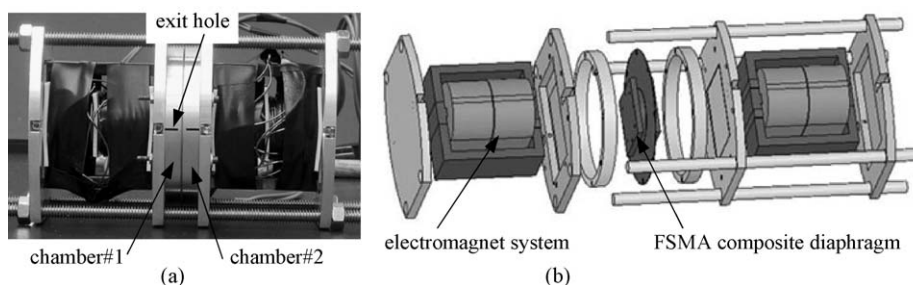

Fig. 7. (a) The photo as assembled membrane actuator, (b) the schematic of actuator parts.
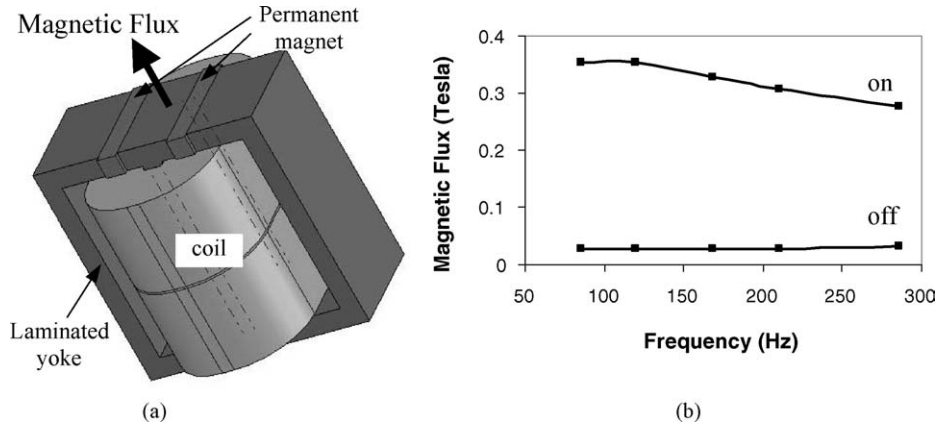
Fig. 8. (a) The schematic of single unit of electromagnet and (b) its magnetic field responses as a function of frequency.

the parts of the FSMA composite diaphragm and the aluminum rings are fixed by screws. Gaskets and silicon are applied to ensure the tight seal of the chamber.

Fig. 8 shows the single unit of electromagnet (about 500 g) and its magnetic field responses (the arrow as shown in Fig. 8(a)) measured by a digital Teslameter (Group 3, DTM133) as a function of frequency. The Teslameter probe is sandwiched between the electromagnet surface and a soft iron pad. The electromagnet consists of laminated yoke, two electrical coils and two permanent magnets (4.78 mm × 4.78 mm × 27 mm each). The overall dimension of the electromagnet without coils is 55 mm × 55 mm × 25 mm. The laminated yoke made by 0.15 mm thick Fe–Si sheets in the electromagnet is to eliminate the eddy current effect for high frequency usage (up to 400 Hz). In order to obtain a fast frequency response of circuit and a strong magnetic flux gradient, two electrical coils (100 turns each) are electrically parallel connected but magnetically series connected. The magnetic polarization of both permanent magnets is opposite to each other and the magnetic flux flows inside the yoke as a close loop. When the electrical current goes through both coils, the magnetic flux will be punched out of the yoke between permanent magnets and create a large magnetic flux gradient. The input current signal is a square wave controlled by a stepping motor controller which is commercial available. Fig. 8(b) shows that when there exists no electrical current, the residual magnetic field is very small around 0.01 T. When the power (4 A, 25 V) goes through coils, the magnetic field can reach 0.35 T with a slight decay as the frequency goes

up to 300 Hz. This will ensure that the membrane actuator can be operated up to 300 Hz.

The synthetic jet flow velocity from the membrane actuator is measured by the hotwire method (TSI IFA 100 with a platinum hot film probe). The probe is carefully located just at the exit hole and parallel to the length of the exit hole. The total input power is 8 A at 25 V. Fig. 9(a) shows the results of jet flow velocities as a function of frequency for three different thickness (0.2, 0.3 and 0.4 mm) of NiTi thin sheet of the composite diaphragm. The velocity increases as the frequency increases and shows the peak of velocity at 200, 220 and 250 Hz, respectively. This trend is associated with the resonance frequency of each composite diaphragm. The maximum jet velocity, 190 m/s at 220 Hz, is obtained by using the 0.3 mm thick NiTi sheet of the composite diaphragm. The jet velocity is much stronger than the jet produced by other types of synthetic jet actuators, i.e., 60 m/s at 260 Hz (260 W) for the voice coil based actuator [10] and 46 m/s at 900 Hz (25 V) for the piezoelectric based actuator [17]. Its displacement-frequency response is shown in Fig. 9(b) which is observed by a high-speed video camera system (KODAK Motion Corder Analyzer, Model 1000SR). Due to the geometric limitation, the standard measurement of dynamic frequency response was not possible. The peak-to-peak displacement reaches maximum of 3.72 mm at the frequency of 190 Hz. The peak frequency difference between the maximum jet velocity and the maximum displacement may be due to the different level of air compression inside the chamber. Based on the performance of 0.3 mm thick composite diaphragm, its
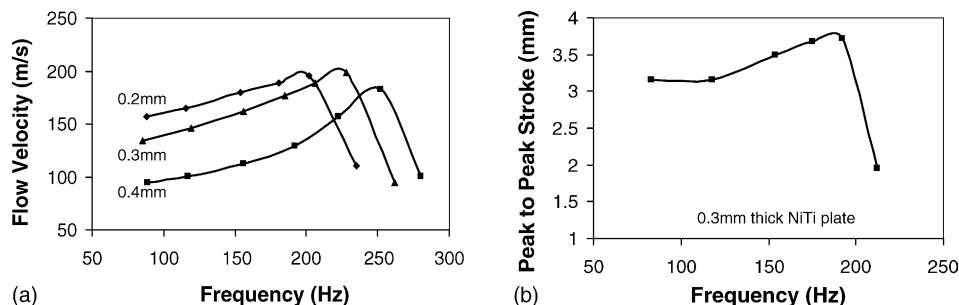

Fig. 9. (a) The synthetic jet flow velocity as a function of frequency produced by three different thickness (0.2, 0.3, 0.4 mm) of NiTi plates and (b) the peak-to-peak displacement of the composite diaphragm (0.3 mm thick NiTi plate).

energy density (ED = work/FSMA composite volume) is calculated as 30 kJ/m^3 and its power density (PD = ED × frequency) is 6000 kW/m^3. These data are important parameters of the FSMA composite performance. If more stroke of the composite diaphragm (faster the jet velocity) can be obtained due to SIM, both ED and PD will further increase. Also the higher the frequency response of the material becomes, the larger PD will be. To consider the performance due to the weight of the driving unit and the power consumption of the membrane actuator, the specific efficiency of the current actuator (work × frequency/(voltage × ampere × total weight of actuator)) is 12 %/kg.

4. Discussions

The membrane actuator is designed based on "hybrid mechanism", i.e., stress-induced martensitic phase transformation (SIM) caused by large force due to large magnetic field gradient, thus enhancing the displacement, as the stiffness of shape memory alloy reduces due to the martensitic transformation. Therefore, the information of the maximum stress level on the composite diaphragm is very important. The larger displacement of the composite diaphragm due to the martensitic transformation, the larger the volume change we can obtain, resulting in a stronger synthetic jet velocity (Eq. (3)). Based on the theory of plate and shell [28], the maximum stress and the maximum displacement can be estimated by

$$\sigma_{\max} = k \frac{P}{h^2} \tag{4}$$

$$w_{\max} = k_1 \frac{Pa^2}{Eh^3} \tag{5}$$

where P is the load, h the thickness, a the radius of diaphragm, w the displacement of the center part of the diaphragm and E is the Young's modulus. We can estimate the displacement of the composite plate before the onset SIM on the NiTi sheet. In the case of 0.3 mm thick NiTi sheet of the composite diaphragm, when the displacement of the center part of the diaphragm reaches 1.5 mm, the NiTi is at the onset of martensitic transformation (450 MPa). Further, the FEA results show that the maximum stress reaches 510 MPa when the displacement of the center part of the diaphragm is 3.72 mm peak-to-peak (at 190 Hz, as shown in Fig. 9(b)). Therefore, the FSMA composite diaphragm induces a strong synthetic jet flow when it goes into the stress-induced martensitc transformation. However, if more SIM is utilized, the membrane actuator can produce a stronger synthetic jet.

Because of lack of information on high frequency cyclic loading on NiTi SMA, the dynamic FEA only serves as a design guidance to allocate the range of resonance frequency of the composite diaphragm. The high strain rate effect on flow stress is an important issue to the design and the performance of the membrane actuator. Although some researchers have reported on the issue of the dynamic loading on NiTi SMA, they mainly focused on the damping capacity at low frequency with either tension or compression loading. The strain rate of a vibrating composite diaphragm (i.e., +2 to −2% strain at 300 Hz) can be as high as 12 s^{-1} which is still far below the level by impact testing. Therefore, to fully understand its frequency responses, it is very important to conduct investigations on the cyclic tension-compression loading of superelatic NiTi SMA at high frequency. In addition, it is necessary to investigate the interfacial bonding of the FSMA composite diaphragm between NiTi and soft iron under the cyclic loading to ensure the fatigue life of metallic bonded FSMA composite.

The gap between estimated and experimentally measured flow velocities (275 and 190 m/s, respectively) could be due to the energy loss of jet flow and the shape of the deformed composite diaphragm. When the jet flow runs through the exit hole, the friction between the wall of the hole and airflow will result in energy loss. More fluid dynamic investigations will be needed to measure the energy loss due to the friction. The jet flow velocity can be calculated by Eq. (3). The estimated volume change due to the deformation of the composite diaphragm is assumed as the corn shape as shown in Fig. 5. However, the kink points of deformed composite diaphragm in the experiment will not be as sharp as shown in Fig. 5. This means that the estimated volume change will be overestimated and it results in the overestimated flow velocity by Eq. (3).

5. Summary

A high performance membrane actuator for synthetic jet applications was successfully designed and constructed based on the FSMA composites and hybrid mechanism. The FSMA composite diaphragm oscillates at high frequency by the electromagnet system, which provides high magnetic field gradient and strong force. The hybrid mechanism is based on the stress-induced martensitic phase transformation produced by applied magnetic field gradient, thus enhancing the displacement, as the stiffness of shape memory alloy reduces due to the martensitic phase transformation. Currently, the actuator can produce the maximum jet velocity of 190 m/s at 220 Hz.

References

[1] B. Smith, A. Glezer, The formation and evolution of synthetic jets, Phys. Fluids 10 (1998) 2281–2297.

[2] L. Pack, R. Joslin, Overview of active flow control at NASA Langley Research Center, Proc. SPIE 3326 (1999) 202–213.

[3] A. Siefert, T. Bachar, D. Moss, M. Shepshelovich, I. Wygnanski, Oscillatory blowing: a tool to delay boundary-layer separation, AIAA J. 31 (11) (1996) 2052–2060.

[4] A. Siefert, A. Darabi, I. Wygnanski, Delay of airfoil stall by periodic excitation, AIAA J. Aircraft 4 (1996) 691–698.

[5] A. Seifert, L.G. Pack, Oscillatory control of separations at high Reynolds numbers, AIAA 98-0214, 1998.

[6] I. Wygnanski, Boundary layer and flow control by period addition of momentum (invited), AIAA 97-2117, 1997.

[7] M. Hites, H. Nagib, T. Bacher, I. Wygnanski, Enhanced performance of airfoils at moderate mach numbers using zero-mass flux pulsed blowing, in: Proceedings of the 39th Aerospace Sciences Meeting and Exhibit, AIAA Paper 2001-0734, Reno, NV, January 12–15, 2001.

[8] A. Honohan, M. Amitay, A. Glezer, Aerodynamic control using synthetic jet, AIAA Fluids, June 2000. AIAA 2000-2401, 2000.

[9] H. Nagib, J. Kiedaisch, D. Greenblatt, I. Wygnanski, A. Hassan, Effective flow control for rotorcraft applications at flight mach numbers, AIAA-2974, 2001.

[10] D. McCormick, S. Lozyniak, D. MacMartin, P. Lorber, Compact, high-power boundary layer separation control actuation development, in: Proceedings of the ASME Fluids Eng. Div. Summer Meeting, vol. 2, 2003, pp. 555–561.

[11] F.T. Calkins, J.H. Mabe, J.P. Smith, D.J. Arbogast, The Boeing Company Phantom Works, Low frequency ($F+ = 1.0$) multilayer piezopolymer synthetic jets for active flow comtrol, AIAA paper, 2002-2823.

[12] F.T. Calkins, D.J. Clingman, Vibrating surface actuators for active flow control, Proc. SPIE 4698 (2002) 85–96.

[13] R. Bryant, R. Fox, J. Lachowicz, F. Chen, Piezoelectric synthetic jets for aircraft control surfaces, Proc. SPIE 3674 (1999) 220–227.

[14] K. Mossi, R. Bryant, Characterization of piezoelectric actuators for flow control over a wing, Actuator (2004) 181–185.

[15] L. Cattafesta, S. Garg, D. Shukla, Development of piezoelectric actuators for active flow control, AIAA 39 (8) (2001) 1562–1568.

[16] P. Mane, K. Mossi, R. Bryant, Synthetic jets with piezoelectric diaphragm, Proc. of SPIE 5761 (2005) 233–243.

[17] Q. Gallas, R. Holman, T. Nishida, B. Carroll, M. Sheplak, L. Cattafesta, Lumped element modeling of piezoelectric-driven synthetic jet actuators, AIAA 41 (2) (2003) 240–247.

[18] S. Ugrina, A. Flatau, Investigation of synthetic jet actuator design parameters, Proc. of SPIE 5390 (2004) 284–296.

[19] M. Sugiyama, R. Oshima, F.E. Fujita, Trans. Jpn. Inst. Met. 27 (1986) 719.

[20] R.D. James, W. Wuttig, Magnetostriction of martensite, Phil. Mag. A 77 (1998) 1273–1299.

[21] H. Kato, T. Wada, Y. Liang, T. Tagawa, M. Taya, T. Mori, Martensite structure in polycrystalline Fe–Pd, Mater. Sci. Eng. A 332 (2002) 134–139.

[22] T. Wada, Y. Liang, H. Kato, T. Tagawa, M. Taya, T. Mori, Structure change and straining in Fe–Pd polycrystals by magnetic field, Mater. Sci. Eng. A 361 (2003) 75–82.

[23] Y. Liang, Y. Sutou, T. Wada, C. Lee, M. Taya, T. Mori, Magnetic field-induced reversible actuation using ferromagnetic shape memory alloys, Scripta Mater. 48 (10) (2003) 1415–1419.

[24] H. Kato, T. Wada, T. Tagawa, Y. Liang, M. Taya, Development of ferromagnetic shape memory alloys based on Fe–Pd alloy and its applications, in: Proceedings of Material Sciences for 21th Century, The Society of Material Science Japan, Col. A, 2001, pp. 296–305.

[25] Y. Liang, T. Wada, T. Tagawa, M. Taya, Model calculation of stress–strain relationship of polycrystalline Fe–Pd and 3D phase transformation diagram of ferromagnetic shape memory alloys, Proc. of SPIE 4699 (2002) 206–216.

[26] K. Oguri, Y. Ochiai, Y. Nishi, S. Ohino, Y. Uchida, Extended Abstracts of 9th Intelligent Materials Forum, Mitoh Science and Tech, Tokyo, March 16, 24–25, 2000.

[27] T. Wada, M. Taya, Spring-based actuators, Proc. of SPIE 4699 (2002) 294–302.

[28] S. Timoshenko, S. Woinowsky-Krieger, Theory of Plates and Shells, 2nd ed., McGraw-Hill, New York, 1987, pp. 61–62.

Biographies

Yuanchang (Robert) Liang is currently working as a research associate in the Center for Intelligent Materials and Systems at the University of Washington, Seattle. He received his B.S. degree from National Taiwan University, Taipei, Taiwan in 1992, M.S. in mechanical engineering from Lehigh University, Bethlehem in 1998 and Ph.D. degree in mechanical engineering from University of Washington in 2002. His current research interests are intelligent materials and their applications.

Yasuo Kuga is a Professor of Electrical Engineering at the University of Washington. He received his B.S., M.S., and Ph.D. degrees from the University of Washington, Seattle in 1977, 1979, and 1983, respectively. From 1983 to 1988, he was a Research Assistant Professor of Electrical Engineering at the University of Washington. From 1988 to 1991, he was an Assistant Professor of Electrical Engineering and Computer Science at The University of Michigan. Since 1991, he is with the University of Washington. He was an Associate Editor of Radio Science (1993–1996) and IEEE Trans. Geoscience and Remote Sensing (1996–2000). He was elected to IEEE Fellow in 2004. His research interests are in the areas of microwave and millimeter-wave remote sensing, high frequency devices and materials, and optics.

Minoru Taya is Boeing-Pennell Professor of Mechanical Engineering at the University of Washington. He has been a Professor of Mechanical Engineering, and Adjunct Professor of Materials Science and Engineering at the University of Washington since 1986. He received a Bachelor of Engineering in 1968 from the University of Tokyo, Japan; Master of Science in Civil Engineering in 1973 and Doctor of Philosophy in Theoretical Applied Mechanics in 1977, both from Northwestern University. He taught at the University of Delaware as an Assistant and Associate Professor from 1978–1985. He has had visiting appointments at the University of Oxford, U.K., Riso National Laboratory, Denmark, University of Tokyo, and Institute of Space and Aeronautical Science, Japan. During 1989–1991 he was Professor of Materials Systems, Department of Materials Processing, Tohoku University, Japan. Dr. Taya serves as Associate Editor for Materials Science and Engineering-A, and ASME Journal of Applied Mechanics, and is currently chair of the Electronic Materials Committee of ASME Materials Division. He is Fellow of ASME, and American Academy of Mechanics, and International Editorial Board member of Advanced Composite Materials. Dr. Taya is currently running a Center for Intelligent Materials and Systems (CIMS) as Director, where he is involved in supervising a number of projects related to intelligent materials and systems. The intelligent materials that he has been studying are piezoelectric composites, shape memory alloys (SMA), ferromagnetic SMA(FSMA), electro- and photo-active polymers, and designed actuators based on these materials. The electroactive polymers (EAPs) include hydrogels such as Nafion and Flemion, and electrochromic polymers. These intelligent materials are the key materials for high performance actuators, ranging from MEMS to artificial muscles.